Soldagem & Inspeção. 2018;23(2):225-234
https://doi.org/10.1590/0104-9224/SI2302.09
ISSN 1980-6973 (Online)
ISSN 0104-9224 (Print)

Technical Papers

Deposition of AA5083-H112 Over AA2024-T3 by Friction Surfacing

Samuel Silvério[1], Hennin Krohn[2], Viktoria Fitseva[2], Nelson Guedes de Alcântara[1], Jorge Fernandez dos Santos[2]

[1] Universidade Federal de São Carlos – UFSCar, Departamento de Engenharia de Materiais, São Carlos, SP, Brasil.
[2] Helmholtz-Zentrum Geesthacht, Institute of Materials Research, Materials Mechanics, Solid-State Joining Processes, Geesthacht, Schleswig-Holstein, Germany.

Received: 09 Apr., 2018
Accepted: 22 June, 2018

E-mails: samuelhsilverio@gmail.com (SS), henning.krohn@hzg.de (HK), viktoria.fitseva@hzg.de (VF), nelsong@ufscar.br (NGA), jorge.dos.santos@hzg.de (JFS)

Abstract: Friction surfacing (FS) is an advanced solid state process in surface modification with increasing applications in reclaiming worn parts, hardfacing and corrosion protection. The advantages of the process are that materials are deposited in the solid state and the resultant forged microstructure which leads to enhanced mechanical properties. As no melting takes place, the process allows joining of dissimilar materials while avoiding several fusion related problems. The present study addresses the deposition of AA5083-H112 coatings over AA2024-T3 substrates focusing on the influence of the main process parameters such as axial force, rotational speed and deposition speed, in the mechanical properties of the deposits. A performance and geometric analysis of the depositions are also presented. Sound aluminum coatings were produced; plastic deformation and heat generation promotes a dynamic recrystallization of the anisotropic consumable rod, resulting in a fine and homogeneous deposit. The coating presented an increase in ultimate tensile strength and failure deformation of 9% and 6%, respectively. Deposition efficiency between 25 and 50% were obtained, with a maximum of 48% average efficiency observed with 800 RPM, 12 kN and 16 mm/s.

Key-words: Friction surfacing; Solid state; Aluminum; AA 5083-H112; AA 2024-T3.

Deposição por Fricção de AA5083-H112 sobre AA2024-T3

Resumo: A deposição por fricção (FS) é um avançado processo de modificação da superfície no estado sólido, com aplicações crescentes na recuperação de peças desgastadas, proteção contra corrosão e revestimento. É considerada uma derivação do processo de soldagem por fricção, mantendo muitos benefícios do processo primário, tais como: fase sólida, microestrutura forjada e excelente ligação metalúrgica. Como não ocorre fusão dos materiais envolvidos, o processo permite a união dissimilar de materiais, evitando vários problemas relacionados com a fusão. O presente estudo aborda a deposição da liga de alumínio 5083-H112 sobre substratos de AA2024-T3, estudando sua viabilidade técnica e focando na influência do processo termomecânico nas propriedades metalúrgicas e mecânicas dos depósitos. Também são apresentados uma análise de desempenho e geométrica das soldas. A deposição das ligas foi realizada com sucesso; A deformação plástica e a geração de calor promovem uma recristalização dinâmica da até então estrutura anisotrópica do bastão consumível, resultando num depósito com microestrutura fina e homogênea, livre de qualquer deformação anterior. O depósito apresentou um aumento na resistência à tração e à deformação de ruptura de 9% e 6%, respectivamente. A eficiência de deposição obtida foi entre 25 e 50%, com um máximo de 48% de eficiência média observada com 800 RPM de velocidade rotacional, 12 kN de forca axial e 16 mm/s de velocidade transversal.

Palavras-chave: Deposição por fricção; Estado sólido; Alumínio; AA 5083-H112; AA 2024-T3.

1. Introduction

Friction surfacing (FS) is an advanced solid-state process in surface modification [1], it was first patented as metal coating process in 1941 by Klopstock and it derives from the friction stir welding process, keeping many benefits of the primary process such as: solid phase, forged microstructure and excellent metallurgical bond [2]. FS is an environmentally clean process with no fumes, spatter or high energy light emissions. It is energy efficient considering the heat is generated exactly where is demanded [3]. Metallurgically incompatible materials can be joined and since the dilution of the coating onto the substrate is negligible, good adhesion can be achieved [4]. Moreover, no occurrence of pores, slag or inclusions are usually observed in the coatings in comparison to traditional processes which involve melting, for instance the arc welding process [5]. Regarding the process, it sometimes demands high forces to be concluded and one disadvantage is the higher stiffness the machine should have.

The friction surfacing process is mostly applied for corrosion and wear resistant coatings and to reclaim worn engineering components [6]. More specific applications include the fabrication of machine knives for the food and pharmaceutical processing and packaging industries, the hardfacing of valve seats with stellite – typical hardfacing alloys which are cobalt-based alloys with high hardness at high temperature and corrosion resistance and high wear resistance under high-pressure conditions, the repair and manufacture of parts for the gas turbine industry and some types of tooling as punches and drills [6].

The process starts when the consumable rod starts to rotate and an axial force is applied in the top of the rod, pressing it tightly against the substrate. The axial force and the rotational speed lead to an intense frictional heat production at the rubbing surface between the substrate and the consumable rod [1]. As the substrate is bigger in volume and it is more efficient in transfer the heat compared to the consumable rod, the heat exchange in the substrate has a higher speed than in the rod. This means that the heat produced concentrates at the bottom end of the rod where a large axial temperature gradient occurs, and not in the substrate itself [1,5]. As a consequence of the friction heat produced, the material of the rod's tip becomes plasticized. Combining the rotational speed and the traverse movement, the material plasticized of the rod is transferred to the substrate in order to form the layer, as can be seen in Figure 1.

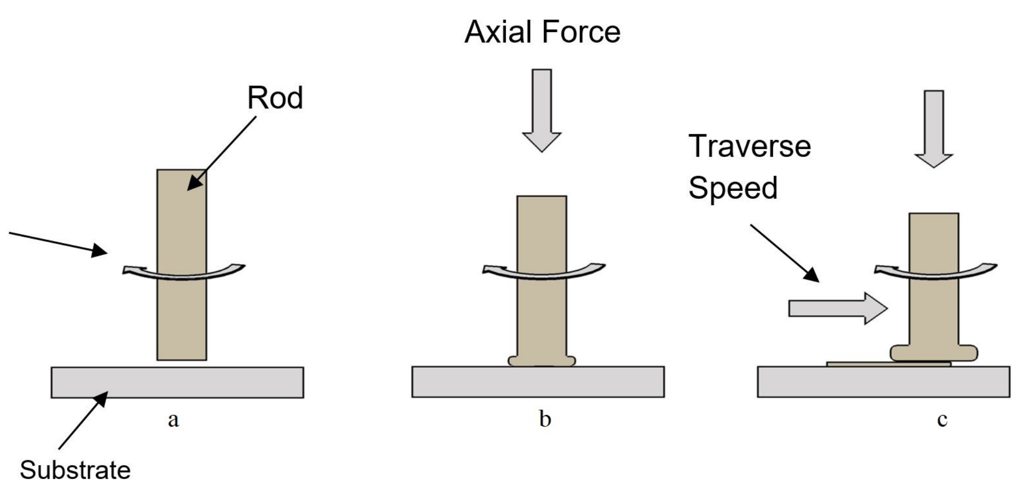

Figure 1. Schematic of FS process described in four steps. (a) Positioning of the consumable rod; (b) plastification phase under axial load and rotational speed; (c) coating is deposited onto the substrate.

Notice that not all the material of the consumable rod is deposited on the substrate as part of the rod is discharged outside which is called "flash". A probable cause for the formation of the flash is the skidding between the consumable rod and the friction surface, which is increased in processes involving higher axial force and rotational speeds [7].

Friction surfacing of some dissimilar alloys were already attempted. Most studies focus on ferrous alloys but there are some investigations with light alloys such as aluminum, as can be seen in Table 1.

Table 1. Friction surfacing combinations deposited over aluminum plates [8,9].

Consumable Rod	Substrate	Author
AA1100	Aluminum	Beyer et al. [10]
AA2017	AA5052	Tokisue et al. [11]
AA5052	AA5052	Sakihama et al. [7]
AA6082-T6	AA2024-T3	Suhuddin et al. [12] / Gandra et al. [13]

The objective of this study is first the feasibility study of this new combination of materials and mainly the investigation of the influence of the thermo-mechanical process in the metallurgical and mechanical properties of the deposits using aluminum alloy 2024-T3 as substrate and aluminum alloy 5083-H112 as a consumable rod.

2. Materials and Methods

The materials used in this study were AA2024-T3 aluminum plates with 2 mm thickness as substrates and 5083-H112 consumable rods with 20 mm diameter. Chemical compositions of both materials are presented in the Table 2.

Table 2. Chemical compositions of the alloys.

Element (wt%)	Cr	Cu	Fe	Mg	Mn	Si	Ti	Zn
AA2024	≤ 0.10%	3.8	≤ 0.50%	1.2%	0.3%	≤ 0.50%	≤ 0.15%	≤ 0.25%
AA5083	≤ 0.25%	≤ 0.10%	≤ 0.40%	4.5%	0.6%	≤ 0.40%	≤ 0.15%	≤ 0.25%

Depositions were performed using rotational speeds of 800, 1000 and 1200min^{-1}, deposition speeds of 12, 14 and 16 mm/s and axial forces of 12, 14 and 16 kN. This set of parameters were chosen based on preliminary tests on a 4 mm substrate.

The equipment used to produce the deposit, through the friction surfacing process can be seen in Figure 2. It basically consists in a consumable stabilization system, which allows it to rotate freely while preventing lateral movement, along with a clamping system of the substrate that will prevent it to move completely. The substrate is attached to the machine table using clamping systems for both sides and the consumable rod is fixed at a device above the table.

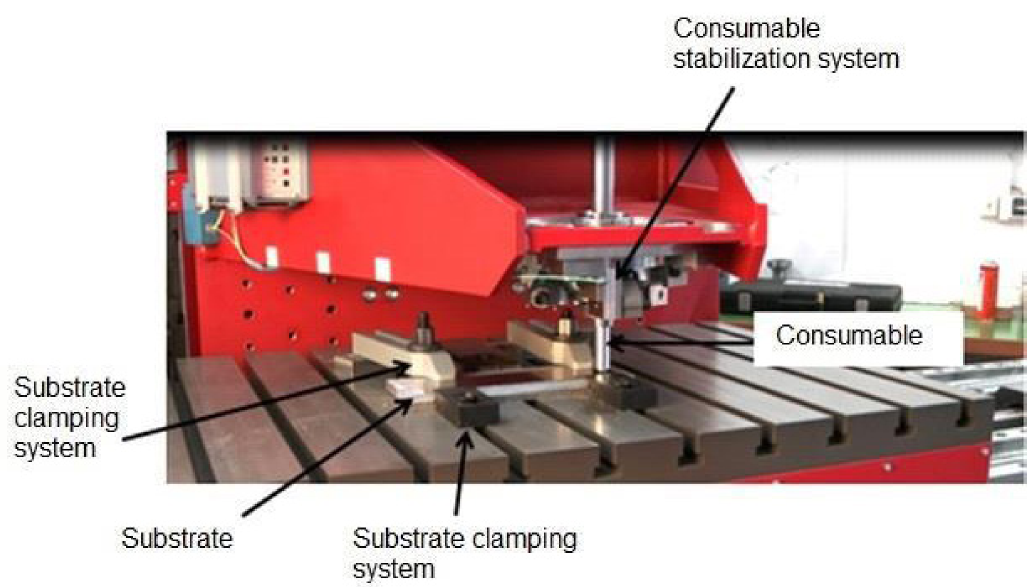

Figure 2. RAS machine used in the friction surfacing process.

Consumable rods and substrates were degreased prior to deposition and operating conditions (forging force, torque, consumable rod consumption, position and deposition speed) were monitored in real time.

The coated samples were cross sectioned, polished and etched with a Keller's reagent for metallographic analysis.

The microhardness tests based on ASTM E384-11 were conducted on the cross section of the substrate and deposit with the aid of a device Zwick / Roell-ZHV using a conventional indenter.

The mechanical properties were obtained by tensile test using micro specimens of the deposit. Allowing a local and precise characterization of the mechanical properties. All micro-specimens were extracted from the layers via electro discharge machining (EDM). The micro-specimens geometry was designed on the basis of standards DIN EN 2002-001:2006-11 and DIN EN ISO 6892-1:2009-12.

3. Results and Discussion

3.1. Metallurgical analysis

The thermo-mechanical process of the friction surfacing consists of high complex transformations, involving joining and hot-working principles. The dynamic recrystallization occurs normally in metals with medium and low stacking fault energy (SFE), where the dynamic recovery is slow and allows the dislocation density to increase to a significant level. When a certain critical density is exceeded, new grains are formed during deformation. Even though the aluminum alloys have a high SFE, the deformation is severe enough to reach a critical dislocation density allowing the dynamic recrystallization process to occur [8,9].

The coating properties are mainly determined by the grain refinement levels and, in the case of heat treatable alloys, precipitate distribution and size. The solid state joining mechanism is controlled by diffusion, plastic deformation can lead to a disruption of the brittle oxide layers, establishing metal to metal contact and enabling the joining process along a small inter diffusion layer [8,14].

As can be seen in Figure 3, the as-received consumable rod microstructure presents an anisotropic grain structure aligned along the extrusion direction. The hot-working process previously described promotes the generation of a viscoplasticized solid state region that is processed into another form and metallurgical condition, this zone results from the combination of plastic deformation and heat generation leading to dynamic recrystallization with the nucleation and growth of a new set of grains.

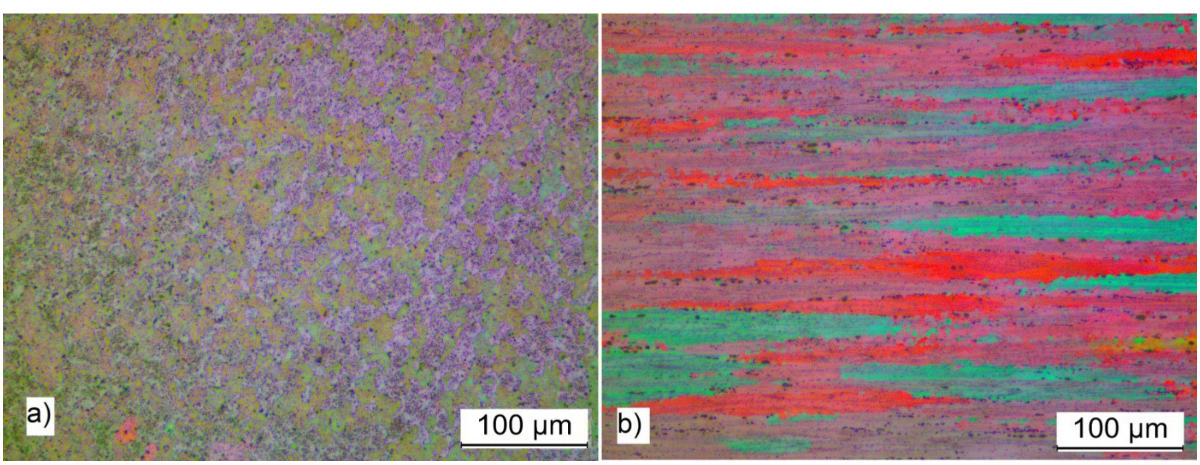

Figure 3. As-received AA5083-H112 consumable rod microstructure: (a) perpendicular to rod extrusion direction; (b) parallel to rod extrusion direction.

Due to this dynamic recrystallization, the coating microstructure appears as a fine and homogeneous new set of grains, free of the previous deformation. All the conditions resulted in the same level of grain refinement. The diffusion bonding interface between the coating and the substrate can be seen in Figure 4.

The highly plasticized material at the tip of the consumable rod is pressed against the substrate without lateral restraint, flowing outside the consumable rod diameter region. This promotes the development of a revolving flash as well as the lack of bonding at the coating edges on both the advancing (rotation and travel movements are in the same direction) and retreating sides (rotation and substrate movement are in opposite directions), as can be seen in the poorly bonded edges in Figure 4. Figure 5 shows one of the successfully deposits of AA 5083 over AA2024.

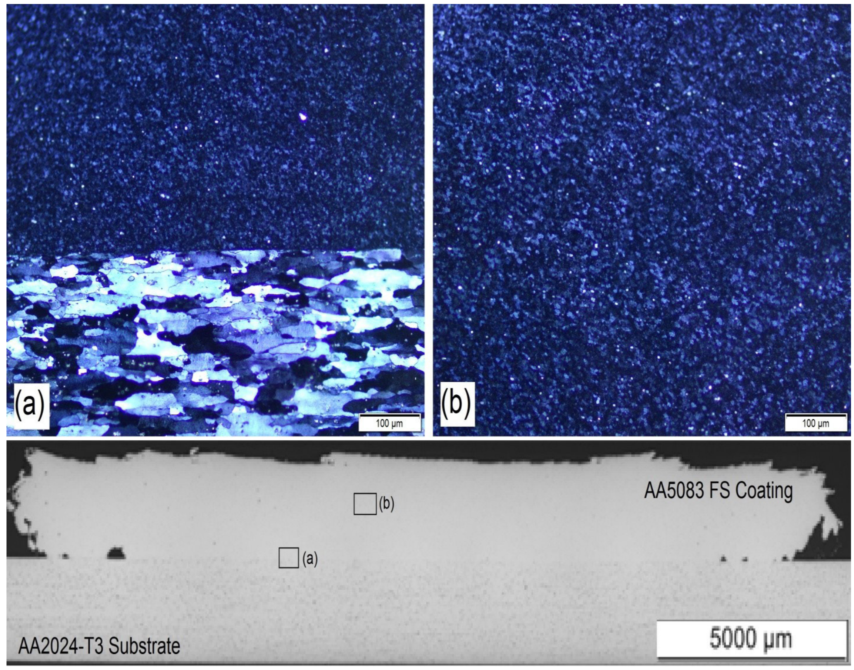

Figure 4. Coating cross section macrograph: (a) bonding interface; (b) coating microstructure.

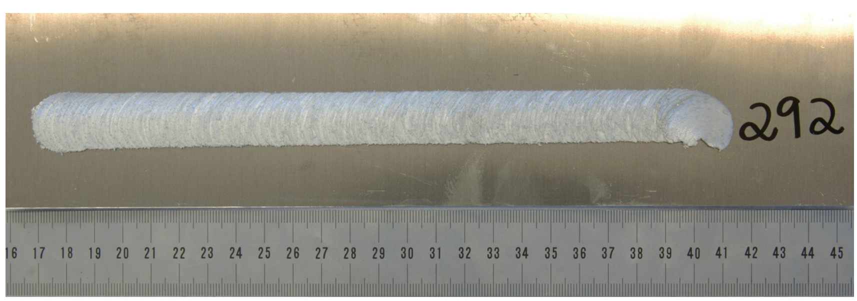

Figure 5. Deposit on the substrate surface by the friction surfacing process for the condition 800 min^{-1}, 12 kN and 12 mm/s.

3.2. Mechanical analysis

The Al-Mg alloys have one commonly observed deformation instability called the Portevin-Le Châtelier effect, that correspond to an instability in the post-yield region at quasi-static loadings (10^-5 – 10^-2 s-1) [15,16]. As can be observed in Figure 6, the PLC behavior manifests in a serrated flow, or stress drops, and is attributed to interactions between dislocations and solute atoms through the phenomenon known as dynamic strain aging. The serrated flow comes from successive dislocation movements and aging while the specimen is deformed. Dislocations can move dragging the solute atoms or they can leave its atmosphere causing the stress drop. Since the mobility of solute atoms is high in the temperatures at which the discontinuous flow occurs, new atoms move to the dislocations, blocking them. The process is repeated many times causing the serrated flow in the stress-strain curves.

Regarding the mechanical properties of the deposits, we were able to notice for all conditions an increase on the yield strength, an increase of 9% on the ultimate strength and an increase of the failure deformation of 6%, comparing to the base material. The average yield strength was 274 MPa, the average ultimate strength was 328 MPa and the average failure deformation was 21,9%. These values were obtained for all conditions with a standard deviation of less than 3 MPa for the strengths and less than 1% for the failure deformation.

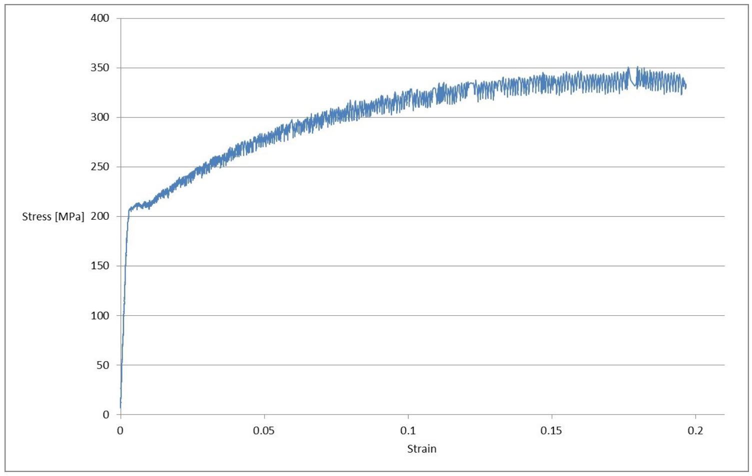

Figure 6. Stress-Strain curve of the deposit achieved for the condition 800 RPM, 12kN and 16mm/s.

As described before, the coating properties are mainly determined by the grain refinement levels. Polycrystalline metals often show a strong dependence of grain size, hardness and resistance. The smaller the grain size, higher the hardness and strength. This occurs because grain boundaries act as obstacles to the dislocation movements, causing stacks of dislocations in their slip plans behind the boundaries. It is assumed that these numbers of dislocations stacks grow with increasing grain size and intensity of the applied tension. Furthermore, these stacks produce a concentration of stresses in the adjacent grain which varies with the number of the dislocations and intensity of the applied tension. Therefore, in materials with coarse-grained the multiplication of tension in the adjacent grain is much higher than in fine grained materials. This means that in fine-grained materials, it will require a much higher tension to cause a dislocation to slip through the boundary than in the case of coarse-grained materials.

As can be seen in the tensile results, this study resulted in a very stable process window which culminates in the same level of grain refinement for all conditions.

The same homogeneous data was observed in the hardness tests, with the average hardness of deposits and substrate of 90.8 and 150 HV0.2 respectively. The indentations were conducted on the middle of the cross section of the substrate and deposit, completely covering the deposit, passing through the heat affected zone and ending at the unaffected substrate. The hardness profile evidences a 0.75 mm deep heat affected zone (HAZ) along the substrate, caused by the heat conducted to the AA2024-T3 substrate, resulting in a slight over ageing marked by a 5% hardness decrease, as can be seen in Figures 7 and 8. The temperatures in the deposition process reach almost the melting temperature of the consumable AA5083, in this case almost 600 °C, which is higher than the solubilization temperature of the substrate AA2024 (495 °C). Therefore, there is a dissolution of precipitates, leading to a decrease in mechanical properties in a localized area of the substrate, the heat affected zone [17].

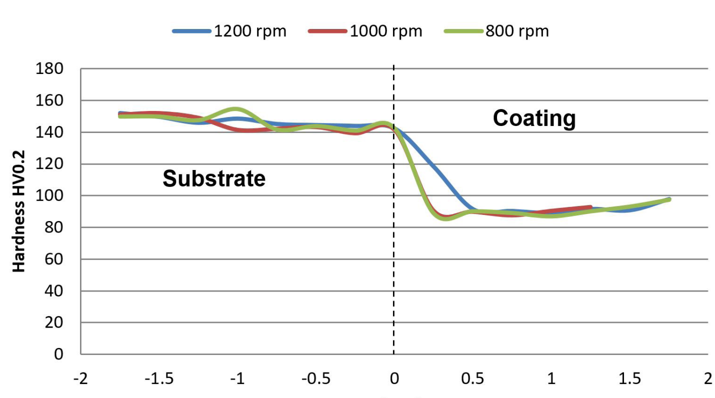

Figure 7. Effect of rotational speed on hardness profile along coating centerline, for the conditions with 12 kN and 12 mm/s.

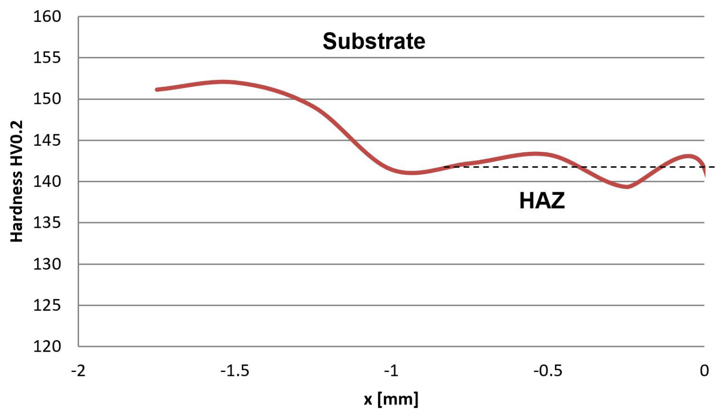

Figure 8. Hardness profile along the substrate showing the heat affected zone, for the condition of 1200 min^{-1}, 14 kN and 14 mm/s.

Gandra observed the same effect on the deposition of AA6082 over AA2024, resulting in the same decrease of hardness but on a 2.2 mm depth. This difference can be explained by the different deposition speeds, since Gandra worked with a lower rotational speed, resulting in a higher heat exposure by the substrate [13].

Since the mechanical properties are stable inside the process window, having almost no variation within the deposition parameters, it is possible to change the geometry of the layer or work with a more efficient condition without interfering in the mechanical properties of the deposits, allowing greater flexibility in the deposition of these dissimilar alloys.

3.3. Influence of process parameters

Coating width and thickness were measure to investigate the effect of process parameters as such as rotational speed, axial force and disposition speed on the geometry of the deposits. All the results were analyzed through a statistical analysis and the results can be seen in Figures 9-11.

Through the statistical analysis it can be observed that the rotational speed has the greatest influence on the geometry of the deposit, higher rotational speeds resulted in a reduction of both coating thickness and width as reported by Sakihama et al. [7].

In higher rotational speeds the contact areas between the consumable rod and the substrate decrease, with that the transfer of friction heat into the substrate becomes smaller, resulting in smaller deposits. The effect of axial force in the process was the same as observed by Gandra et al. [13] and Shinoda et al. [18] where higher

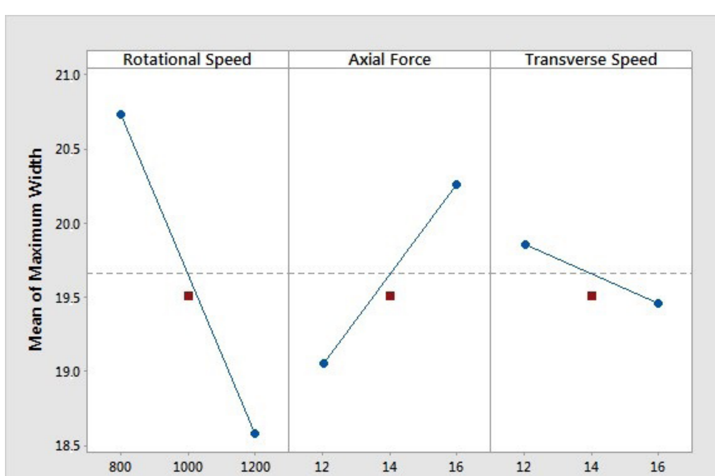

Figure 9. Main effects plot for maximum width.

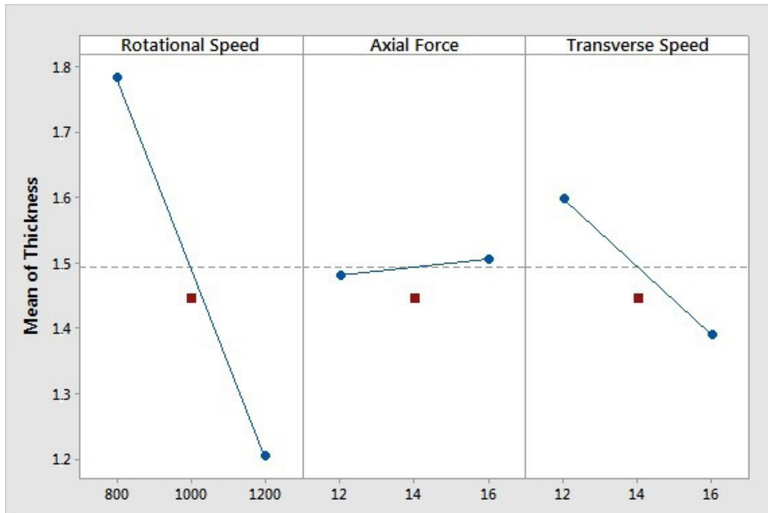

Figure 10. Main effects plot for thickness.

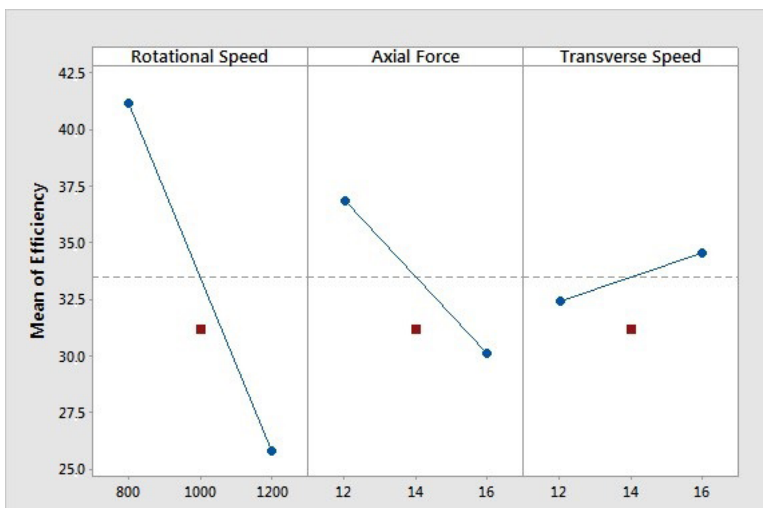

Figure 11. Main effects plot for efficiency.

axial forces resulted in an increase of the effectively bonded width, increasing from an average of 15,2 mm using 12 kN to 16,6 mm with 16 kN, while led to wider deposits [13,18]. The deposition speed also strongly influences the coating thickness and width since it controls the deposition rate of the process. Therefore, when increased the coating thickness and width reduces proportionally because the amount of plasticized material available is smaller with higher deposition rates [13].

The biggest problem in the efficiency of FS is the flash formation, as can be seen in Figure 12, the highly plasticized material at the tip of the consumable rod is pressed against the substrate without lateral restraint, flowing outside the consumable rod diameter region, promoting the development of a revolving flash as well as the lack of bonding at the coating edges. The lower rotational speed and axial force must promote a better stabilization of the deposition layer avoiding a large flash formation.

Sakihama et al. [7] reported efficiencies from 20 to 40% in the depositions by surfacing of similar and dissimilar combinations of aluminium alloys, these values are slightly lower than that obtained in the present study. Deposition efficiency between 25 and 50% were obtained. The best result observed was with 800RPM, 12kN and 16mm/s, with a 48% average efficiency.

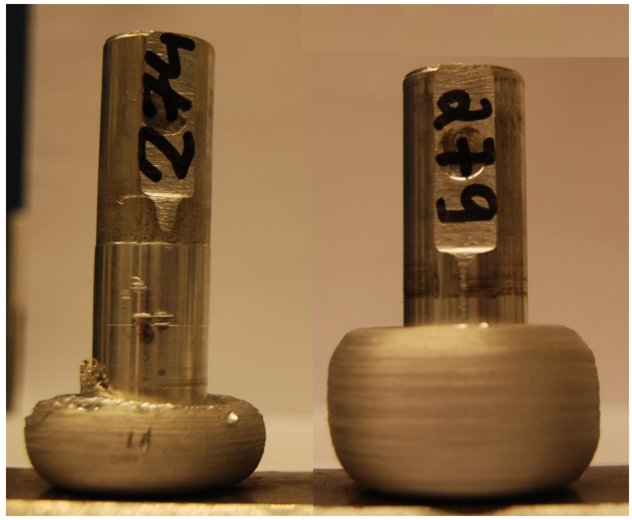

Figure 12. Consumable rods after the process showing the differences between flash formations. Left – 800 min^{-1}, 12 kN and 16 mm/s. Right – 1200 min^{-1}, 16 kN and 12 mm/s.

4. Conclusions

From the present work the following can be concluded:

- AA5083 was successfully deposited on AA2024 by friction surfacing;
- The interface, formed by a solid-state diffusion bonding mechanism, had no porosity and no significant formation of intermetallics was observed;
- The plastic deformation and heat generation promote a dynamic recrystallization of the anisotropic consumable rod, resulting in a fine and homogeneous deposit, free of any previous deformation;
- The hardness profile evidences a 0.75 mm deep HAZ along the substrate, caused by the heat conducted to the AA2024-T3 substrate, resulting in a slight over ageing marked by a 5% hardness decrease;
- Duo to grain refinement, the coating presented an increase in ultimate tensile strength and failure deformation of 9% and 6%, respectively;
- Rotational speed has the greatest influence on the geometry of the deposit with higher rotational speeds resulting in thinner and narrower deposits. Higher axial forces improve bonded width. The transverse speed has an inverse proportionality with the deposit geometry, when increased the coating thickness and width reduces proportionally;
- Deposition efficiency between 25 and 50% were obtained, with a maximum of 48% average efficiency observed with 800RPM, 12kN and 16mm/s. The deposition efficiency decreased with the increase of rotational speed and axial force.

References

[1] Liu XM, Zou ZD, Zhang YH, Qu SY, Wang XH. Transferring mechanism of the coating rod in friction surfacing. Surface and Coatings Technology. 2008;202(9):1889-1894. http://dx.doi.org/10.1016/j.surfcoat.2007.08.024.

[2] Chandrasekaran M, Batchelor AW, Jana S. Friction surfacing of metal coatings on steel and aluminum substrate. Journal of Materials Processing Technology. 1997;72(3):446-452. http://dx.doi.org/10.1016/S0924-0136(97)00209-4.

[3] Vitanov VI, Voutchkov II, Bedford GM. Decision support system to optimize the Frictec (friction surfacing) process. Journal of Materials Processing Technology. 2000;107(1-3):236-242. http://dx.doi.org/10.1016/S0924-0136(00)00710-X.

[4] Nicholas ED. A review of friction processes for aerospace applications. International Journal of Materials & Product Technology. 1998;13(1):45-55.

[5] Fukakusa K. Real rotational contact plane in friction welding of different diameter materials and dissimilar materials: fundamental

study of friction welding. Welding International. 1997;11(6):425-431. http://dx.doi.org/10.1080/09507119709451991.

[6] Vitanov VI, Voutchkov II. Process Parameters selection for friction surfacing applications using intelligent decision support. Journal of Materials Processing Technology. 2005;159(1):27-32. http://dx.doi.org/10.1016/j.jmatprotec.2003.11.006.

[7] Sakihama H, Tokisue H, Katoh K. Mechanical properties of friction surfaced 5052 Aluminum Alloy. Materials Transactions. 2003;44(12):2688-2694. http://dx.doi.org/10.2320/matertrans.44.2688.

[8] Gandra J, Krohn H, Miranda RM, Pereira D, Vilaça P. Friction surfacing: a review. Journal of Materials Processing Technology. 2013;214(5):1062-1093. http://dx.doi.org/10.1016/j.jmatprotec.2013.12.008.

[9] Gandra J, Pereira D, Miranda RM, Silva RM, Vilaça P. Deposition of AA6082-T6 over AA2024-T3 by friction surfacing: mechanical and wear characterization. Surface and Coatings Technology. 2013;223:32-40. http://dx.doi.org/10.1016/j.surfcoat.2013.02.023.

[10] Beyer, M., Resende, A., Santos, J.F. Friction surfacing for multi-sectorial applications (FRICSURF). Geesthacht: Institute for Materials Research, GKSS Forschungszentrum Geesthacht GmbH; 2003. Technical report.

[11] Tokisue H, Katoh K, Asahina T, Usiyama T. Mechanical properties of 5052/2017 dissimilar aluminum alloys deposit by friction surfacing. Materials Transactions. 2006;47(3):874-882. http://dx.doi.org/10.2320/matertrans.47.874.

[12] Suhuddin U, Mironov S, Krohn H, Beyer M, Dos Santos JF. Microstructural evolution during friction surfacing of dissimilar aluminum alloys. Metallurgical and Materials Transactions A, Physical Metallurgy and Materials Science. 2012;43(13):5224-5231. http://dx.doi.org/10.1007/s11661-012-1345-8.

[13] Gandra J, Pereira D, Miranda RM, Vilaça P. Influence of process parameters in the friction surfacing of AA6082-T6 over AA2024-T3. New York: Elsevier B.V.; 2013.

[14] Shirzardi AA, Assadi H, Wallach ER. Interface evolution and Bond strength when diffusion bonding materials with stable oxide films. Surface and Coatings Technology. 2001;31(7):609-618.

[15] Joshi SP, Eberl C, Cao B, Ramesh KT, Hemker KJ. On the occurrence of Portevin-Le Châtelier instabilities in ultrafine-grained 5083 Aluminum alloys. Experimental Mechanics. 2009;49(2):207-218. http://dx.doi.org/10.1007/s11340-008-9208-3.

[16] Robinson JM, Shaw MP. Microstructural and mechanical influences on dynamic strain aging phenomena. International Materials Reviews. 1994;39(3):113-122. http://dx.doi.org/10.1179/imr.1994.39.3.113.

[17] Nicholas ED. A review of friction processes for aerospace applications. International Journal of Materials & Product Technology. 1998;13:45-55.

[18] Shinoda T, Li JQ, Katoh Y, Yashiro T. Effect of process parameters during friction coating on properties of non-dilutional coating layers. Surface Engineering. 1998;14(3):211-216. http://dx.doi.org/10.1179/sur.1998.14.3.211.